

Article

CHMM Object Detection Based on Polygon Contour Features by PSM

Shufang Zhuo^{1,*} and Yanwei Huang²¹ College of Automation Engineering, Fujian Polytechnic of Information Technology, Fuzhou, 350003, China² College of Electrical Engineer and Automation, Fuzhou University, Fuzhou, 350116, China

* Correspondence: zhuo_sf@163.com(S.Z.)

Abstract: Since the conventional split-merge algorithm is sensitive to the object scale variance and splitting starting point, a piecewise split-merge polygon approximation method is proposed to extract the object contour features. Specifically, the contour corner is used as the starting point for the contour piecewise approximation to reduce the sensitivity of the contour segment on the starting point; then, the split-merge algorithm is used to implement the polygon approximation for each contour segments. Both the distance ratio and the arc length ratio instead of the distance error are used as the iterative stop condition to improve the robustness to the object scale variance. Both the angle and length as two features describe the shape of the contour polygon, and affect each other along the contour order relationship. Since they have a strong coupling relationship. To improve the description correction of the contour, these two features are combined to construct a Coupled Hidden Markov Model to detect the object by calculating the probability of the contour feature. The proposed algorithm is validated on ETHZ Shape Classes and INRIA Horses standard datasets. Compared with other contour-based object detection algorithms, the proposed algorithm reduces the complexity of contour description, improves the robustness of contour features to scale variance, and has a higher object detection rate.

Keywords: object detection; contour; polygonal approximation; piecewise split-merge algorithm; Coupled Hidden Markov Model

1. Introduction

Object detection is one of the hotspots and difficulties of computer vision researches, which is the basic technology of high-level vision tasks [1]. Compared with the object detection algorithm based on deep learning, the sample size and computation complexity of the contour-based object detection algorithm are relatively small and low hardware consume. Therefore, the relevant research is getting attention significantly in recent years [2–7]. Detection algorithm used shape as a feature to accurately detect and identify objects and was applied to the visual system of indoor mobile robots [8]. However, there are still many challenges in the contour detection algorithm. The performance of the detection algorithm is susceptible to noise, feature dimensions, and feature descriptors. The robust Hausdorff distance is used to evaluate the similarity between the model feature point set and the object feature point set [9]. However, it is sensitive to noise and only suitable for objects with smooth surface boundaries. In order to improve the robustness to noise, the contour shape is segmented, and each contour segment is matched by constellation shape analysis to improve the feature robustness in the clutter image [10]. However, the computational complexity is increased greatly. The contour edges are fragmented to locally match the object contour model in ergodicity [11]. This method improved the object detection correction under clutter background or occlusion conditions. These methods improve the anti-noise robustness by from point set feature matching to segment feature matching. The Hough transform is used to extract the straight line segment of the warship contour to calculate the turn angle among adjacent straight line segments [12]. The angles are used as feature to establish a hidden Markov model for object detection. This method takes the angle as a contour feature to detect an image with a simple background. In order to enhance the feature expression for the object contour, the angle, distance and arc length

chord ratio are used as the contour descriptor for local matching to improve the object detection accuracy in the clutter background image [6]. Therefore, the technique combining straight line segments with angles is a more efficient method for contour-based object detection. In image processing, the polygon approximation method is often used to replace the curve with multiple line segments to simplify the contour model, and still reserve the key information of the contour. The contour feature of the polygon approximation is more robust to image noise than the point set feature in [9], and has a higher feature matching efficiency. The polygon approximation method for the contour feature is proposed to extract two variables as the angle and the length to improve the anti-interference ability and reduce the contour model complexity.

Since the split-merge algorithm (SM) can well reserve the basic contour features, it is widely used in the industrial production field [13]. SM is sensitive to both the scale variance of the object and the starting point of the split. A modified piecewise split-merge (PSM) polygon approximation algorithm is proposed to improve the SM robustness for the object scale variance and starting point. Specifically, the sharpness is used to detect the corners of object contour as the starting points [14]. The corner sequences are used to segment the object contour as piecewise contours. Each contour segment is approximated by SM algorithm to extract the features of the angle and length. Both the distance ratio and the arc length ratio instead of the distance error are used as the iterative stop condition for SM to improve the robustness to the object scale variance.

In order to improve the matching efficiency of the contour-based object detection algorithm, the hidden Markov model is introduced into the classification process [12,15–17] to achieve good performance. Coupled Hidden Markov Model (CHMM) is used to describe the existence of multiple probabilistic models of interrelated random processes [18]. CHMM not only has the characteristics of Hidden Markov Model (HMM), but also can describe the interdependence between associated stochastic processes, and it is already applied for fault detection [19]. Considering the correlation between the length of the polygon segment and the angle, PSM-based CHMM (PSM-CHMM) is introduced to detect objects. PSM is used to extract the feature variables of the angle and length for object detection and CHMM is used as the object detector with the two features to increase the detect accuracy.

2. Polygon contour feature extraction

The global probability boundary algorithm (gPb) is used to segment the image and extract the object contour [20]. gPb considers the image color, grayscale, texture and other information to extract high-quality image contour. Fig. 1 is the contour of the cup image extracted by the gPb algorithm. The object contours with different detail can be obtained with different thresholds k . Polygon approximation is used to extract the contour features.

PSM polygon approximation algorithm is proposed to extract contour features. Firstly, the corner detection algorithm based on sharpness is used to determine the contour corner, and the contour is segmented by the corner, which reduces the dependence of the contour segment on the starting point. Secondly, PSM algorithm is used to approximate each contour segment. The distance ratio and arc length ratio are used to replace the distance error as the iterative stop condition, which improves the robustness of the object scale variance, such as the size, rotation, etc. Finally, both the angle and length extracted on the approximate polygon as two features describe the contour shape.

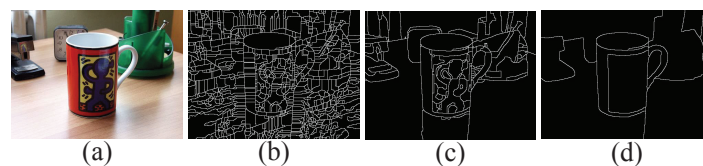


Figure 1. Comparison of results of contour extraction methods. (a)Original image, (b) $k=0.01$, (c) $k = 0.3$, (d) $k = 0.6$.

2.1. Contour piecewise by sharpness-based corner

SM usually performs polygon approximation on the entire contour, and can well reserve the key feature information of the contour. However, starting points would not keep invariable when the object contour is affected by the distance, such as image noise, object rotation, occlusion, and scale variance. The different starting points will result in difference SM results. In order to reduce the difference of contour approximation results, a method of extracting features following segmenting the contours to improve the robustness of clutter image recognition [10]. The starting point is the key technology for contour segmentation. A method to detect the corner is proposed by calculating the sharpness of each point on the contour line with non-maximal suppression [14]. Based on the contour by the sharpness, a contour segmentation method is proposed by detecting the contour corners as starting points of contour segments. This method to detect corners by the sharpness has strong anti-interference ability, small calculation amount and accurate positioning. Every contour segment is estimated by the polygon approximation with SM to extract the features.

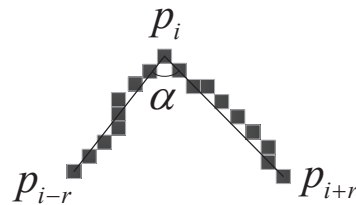


Figure 2. The support angle of point on contour.

Let p_i denote the pixel points on the contour in Fig.2. The support area is defined as, the contour point p_i is given as the center, the center p_i contour segment consists of r ordered former points, p_{i-1}, \dots, p_{i-r} and r ordered rear points, p_{i+1}, \dots, p_{i+r} . These $2r + 1$ points are called as the support region of the point p_i . In Fig. 2, the line segments $p_i p_{i-r}, p_i p_{i+r}$ are support arms, and α is the support angle in the support area. Since the support region is a very small area, the support angle α can be approximated,

$$\sin(\alpha/2) = \frac{|p_{i-r} p_{i+r}|}{|p_i p_{i-r}| + |p_i p_{i+r}|} \quad (1)$$

where the symbol $| \cdot |$ is the module. The sharpness η_i of the point p_i is defined,

$$\eta_i = 1 - \frac{|p_{i-r} p_{i+r}|}{|p_i p_{i-r}| + |p_i p_{i+r}|} \quad (2)$$

The larger η_i , the sharper the angle is. The sharpness η_i is calculated for each point on the contour. When $\eta_i > T$, it is marked as a candidate corner with a set threshold T . The sharpness is,

$$\eta_i = \max_{|j-i| \leq r} \eta_j \quad (3)$$

The higher sharpness, the better the robustness of the point is. The parameter r and the threshold T are selected by the bending degree of the contour. r is generally set to 3~15, and T is generally set to 0.05~0.15. Here, T and r is selected as, $T = 0.05$, $r = 13$. The corner is detected as the starting point of the contour polygon segment approximation. Fig. 3 is the contour segmentation by the corner for the object bat in the MPEG-7 data set. Fig. 4 is the bat divided into two parts to simulate different degrees of occlusion. Both Fig.3 and Fig.4 show that the segmentation of the remaining contours is not affected for either the contour incompleteness or not. So, the segmentation method has a good robustness of the corner detection.

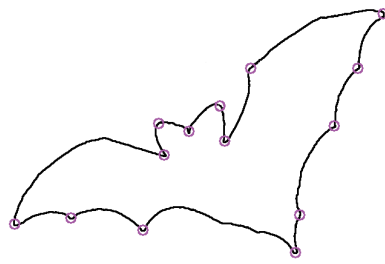


Figure 3. Contour segmentation by corner.

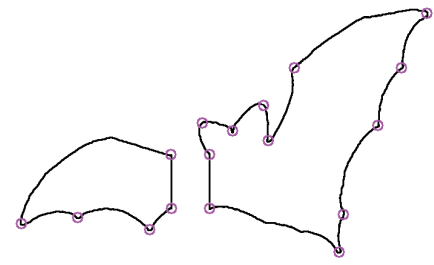


Figure 4. Incomplete contour segmentation.

2.2. PSM polygonal approximation algorithm

When the contours are segmented into segments by corners, each contour segments is estimated by the SM polygon approximation algorithm. The variance of contour starting point does not affect the subsequent contour segments for the polygon approximation, by compared with the approximation method of the entire contour. However, the distance threshold is used as the iterative stop condition for SM algorithm, which results in the different number of vertices for polygons when the object scale varies. In order to improve the robustness of scale variance for SM algorithm, the distance ratio and the arc length ratio as the stopping condition instead of the distance threshold are applied into PSM algorithm. Fig. 5 is the process of PSM polygon approximation algorithm.

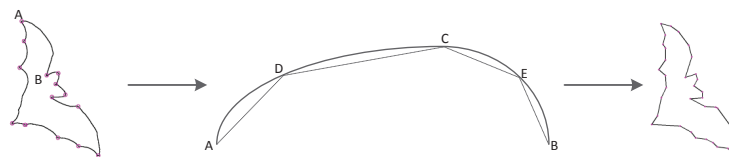


Figure 5. PSM polygon approximation.

Fig. 6 is the basic principle of PSM Polygon approximation algorithm. Let p_1, p_2, \dots, p_n be the sequence of pixel points for a given contour, the point $p_1 = (x_1, y_1)$ is the starting point A, pixel $p_n = (x_n, y_n)$ is the ending point B. The two points A and B are connected as the initial approximation line segment. The length of line segment AB is d_0 , the arc length of contour AB is l_0 , the distance d_i of the point p_i to the line segment AB is calculated in turn to select the pixel point C corresponding to the maximum distance d_{max} . It can obtain the length l_c of the AC arc. The distance ratio d_{max}/d_0 and the arc length ratio l_c/l_0 are used as the stopping conditions for PSM polygonal approximation algorithm. If it satisfies the stopping condition,

$$d_{max}/d_0 < \varepsilon_1 \cup l_c/l_0 < \varepsilon_2 \quad (4)$$

the split stops. If it satisfies the condition,

$$d_{max}/d_0 > \varepsilon_1 \cap l_c/l_0 > \varepsilon_2 \quad (5)$$

the split continues. The pixel points A and C are considered as the starting point and the end point, and the pixel points B and C are considered as the starting point and the ending point, respectively. The splitting process is performed again until the stopping condition satisfies Eq. (4).

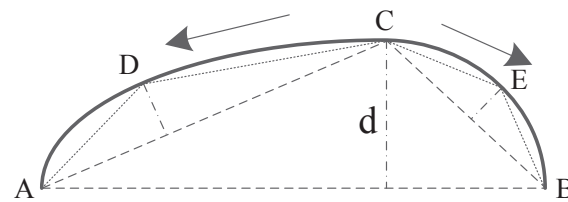


Figure 6. PSM Polygon approximation.



Figure 7. Original image.

The SM algorithm uses the distance as the stopping condition. The distance is an absolute physical quantity. When the contour scale varies, the threshold needs to be adjusted to obtain the approximation result of the same number of vertices. The ratio stop condition of PSM algorithm is a relative physical quantity, and the number of polygon vertices will keep consistent even if the object scale varies.

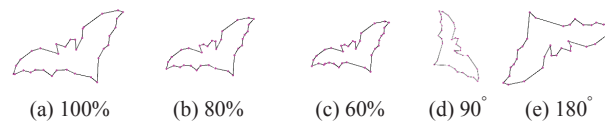


Figure 8. PSM approximation algorithm.

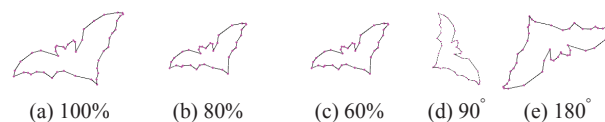


Figure 9. SM approximation algorithm.

Case 1: polygon vertices number comparison for completed contour. PSM and SM (Ramer et al. [13]) algorithm are applied to approximate the bat contour, respectively. The bats are included in the MPEG-7 data set. Fig. 7 (a) is the original image, Fig. 7 (b) is of 80% size of bat, Fig. 7 (c) is of 60% size, Fig. (d) is rotated by 90° clockwise, and Fig. (e) is rotated by 180 clockwise. Fig. 8 and Fig. 9 compare the approximation results of SM algorithm and PSM algorithm. Table 1 shows the number of polygon vertices.

Table 1. Comparison of the number of polygon vertices.

Algorithm	Threshold	100%	80%	60%	90°	180°
SM	2	76	65	58	74	71
SM	4	45	40	36	45	45
PSM	0.03 0.03	36	35	35	35	34
PSM	0.03 0.03	26	26	26	26	26

In Table 1, when the object scale varies and rotates, the number of vertices increases gradually under the same threshold for SM algorithm and keeps almost invariant for PSM algorithm. Compared to SM, PSM improves the robustness of scale variance for the ratio of distance ratio and arc length as the stopping conditions.



Figure 10. Incomplete contours approximation result.

Case 2: the location comparisons of polygon vertices for incomplete contour by PSM. In Fig. 10, bat is divided into two parts. They are fitted by the polygon approximation with PSM, respectively. The location of polygon vertices in each part is consistent with the approximation of the complete contour. So, PSM algorithm cannot affect the location of polygon vertices for either the complete contour or not.

2.3. Contour feature

After the contour polygon is obtained by PSM algorithm, polygon feature variables are extracted as contour descriptors. The angle of the line segment is used as the contour feature of the warship for object detection in the satellite image [12]. The length and angle of the line segment are the two major elements that determine the shape of the polygon. These two feature variables determine the unique shape of the polygon, and the direction of the line segment. But the changes of the two variables are random and asynchronous. In Fig. 11, polygon consists of a set of directed line segments with the angle and length. They are the two necessary factors to describe a directed line segment. Therefore, the polygon contour feature variable is determined as: the angle between the line segment length and the adjacent line segment. Let $P_1, P_2, \dots, P_k, \dots, P_n$ be the ordered polygon vertices for a given contour S , n is the number of the polygon vertices. $\vec{a} = \overrightarrow{P_{k-1}P_k}$, $\vec{b} = \overrightarrow{P_kP_{k+1}}$ indicates two adjacent directed line segments. The angle between the adjacent line segments θ_k is calculated by,

$$\theta_k = \text{sign}(\vec{a} \times \vec{b}) \arccos\left(\frac{\vec{a} \cdot \vec{b}}{|\vec{a}| \cdot |\vec{b}|}\right) \quad (6)$$

The length of the directed segment is $L_k, k = 1, 2, \dots, n$. The length and the angle are normalized to improve the robustness to the scale variance. The descriptor D_S of the contour S is,

$$D_S = \begin{bmatrix} \theta_1 & \dots & \theta_n \\ L_1 & \dots & L_n \end{bmatrix} \quad (7)$$

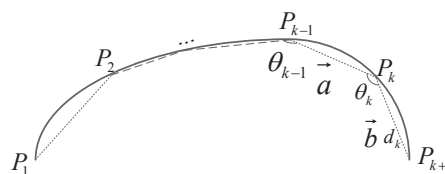


Figure 11. Polygon of the angle and length.

In order to verify the consistency of the length and angle feature extracted by the PSM polygon approximation algorithm, Fig. 12 is the two feature quantity curves along the contour. The length L_k and the angle θ_k sequence of the object in Fig. 7(a)(c)(d) are extracted

by PSM algorithm and SM algorithm, respectively. The threshold of SM algorithm is 4. The threshold of PSM algorithm is $\varepsilon_1 = 0.03$ and $\varepsilon_2 = 0.03$ in Eq.(4).

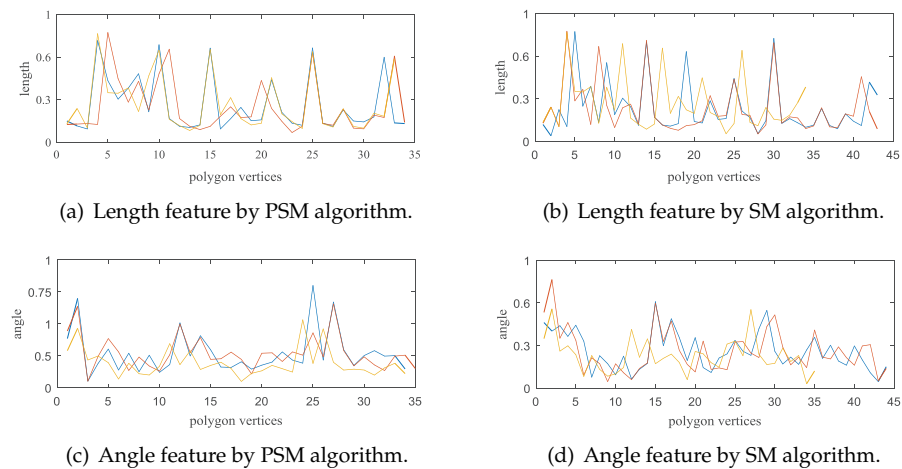


Figure 12. Comparison of the feature curves.

Fig. 12 (a) and (c) are the curves of the length and angle sequences extracted by the PSM algorithm for the bat with the three scales of 100%, 60% and 90°. Fig. 12(b) and (d) are the curves extracted by SM algorithm. The curves have a higher degree of coincidence and reflects the better consistency of the features extracted by PSM algorithm than SM algorithm, since PSM polygon approximation algorithm is more robust to scale variance. Moreover, the trends of the two features extracted on the same contour are asynchronous. So the two features of angle and length, would describe the contour polygon more correctly.

3. Experiment and result analysis

3.1. CHMM

HMM has been applied in object detection, and shows good rapidity and robustness, especially in contour-based object detection research [12,15–17]. HMM is typically trained with a single feature of the object contour. Since the structure of HMM is a single-state Bayesian network, HMM is not suitable for multi-feature models. As contour descriptors, the length and the angle are used to determine the unique shape of the polygon. They have strong coupling relationship, but their trends on the same contour are different and random. For the feature coupling, CHMM with two contour features is constructed to improve the accuracy of object detection and anti-noise robustness.

CHMM has two processes, one is the training process, and the other is the testing process. For the training process, the two features of angle and length are extracted by PSM algorithm for the training image. CHMM is trained with the two features by EM algorithm proposed in Ref[21] to obtain the classifier set $E = \lambda_i$, i is the number of categories. The larger the number of hidden states, the more accurate the model is, but the training efficiency will be lower. In practice, the number of hidden states is 4. In the process of parameter reevaluation, EM algorithm is iterated continuously to increase $P(O|\lambda)$ until $|\log(P_{j+1}(O|\lambda) - P_j(O|\lambda))| < \tau$, j is the iteration number. For the testing process, PSM algorithm extracts the contour polygon feature sequence for the object contour of the test image. The forward-backward algorithm is used to calculate the probability $P(O|\lambda_i)$, i is the object category number, O is the contour feature sequence. The object is identified to the given category by the rule of maximal probability, which must larger than the given threshold.

3.2. Experimental results

In the experiment, the standard data set ETHZ Shape Classes and INRIA Horses were selected to verify the performance of PSM-CHMM. ETHZ Shape Classes contains

255 images of 5 categories of objects, including 40 Apple logos, 48 Bottles, 87 Giraffes, 32 Swans, and 48 Mugs. The half images for every category as the training sets are used to extract the contour feature sequence. The other half images are used as test sets. The INRIA Horses Dataset is the horse images in different scenes, including 170 images with horses and 170 images without horses. 50 images with horses are used as the training set, the other rest images are used as the testing set. For the feature extraction process, the PSM threshold is $\varepsilon_1 = \varepsilon_2 = 0.03$. For the training process, The CHMM parameters are estimated by the EM algorithm. $P(O|\lambda)$ is considered to converge to the maximal value, when the $P(O|\lambda)$ increment of the estimated model parameters for two consecutive times satisfies $|\log(P_{j+1}(O|\lambda) - P_j(O|\lambda))| < 0.001$ to stop the training process. In the experiment, the single-chain θ -HMM and the L -HMM were trained with only one angle and length features for object detection, respectively. Bounding box is the smallest external rectangle of the contour. The performance of PSM-CHMM also compares with the two contour-based methods by Ferrari [1,7]. The indexes of Detection Rate/False-positive (DR/FPPI) per image are used to verify the performance. Fig. 13 is the DR/FPPI curves for the six categories of objects in the ETHZ Shape Classes and INRIA Horses data sets. Table 2 is comparisons of detection rates for 0.3/0.4 FPPI on ETHZ shape classes and INRIA Horses.

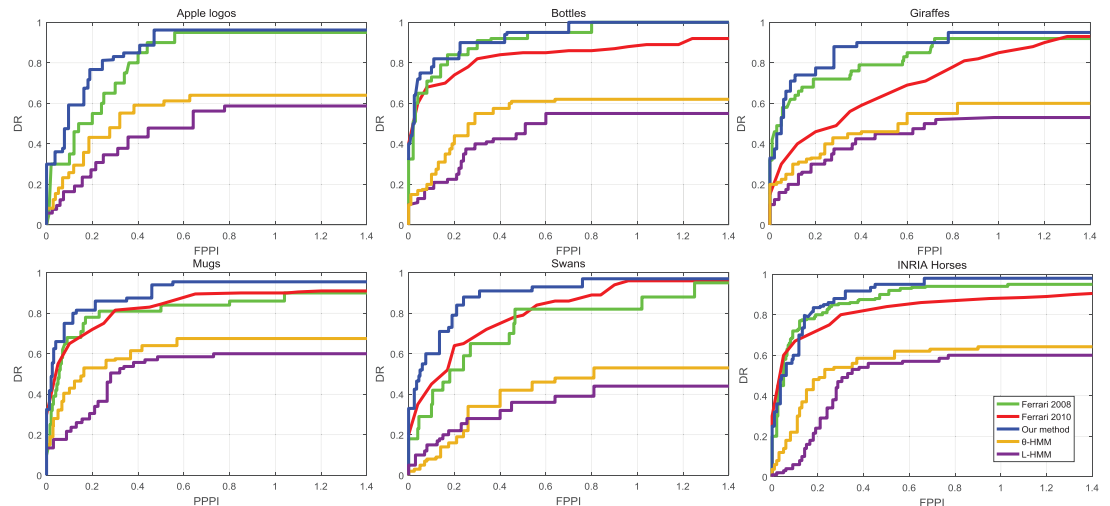


Figure 13. Comparison of DR/FPPI curves on ETHZ shape classes and INRIA Horses.

Table 2. DR comparisons when FPPI = 0.3/0.4.

	θ -HMM	L -HMM	Ferrari 2010	PSM-CHMM
Apple logos	0.62/0.63	0.56/0.6	0.777/0.832	0.826/0.84
Bottles	0.501/0.51	0.38/0.42	0.798/0.816	0.91/0.93
Giraffes	0.36/0.426	0.328/0.34	0.399/0.445	0.833/0.854
Mugs	0.545/0.59	0.49/0.51	0.751/0.8	0.926/0.933
Swans	0.35/0.37	0.32/0.4	0.632/0.705	0.87/0.905
INRIA Horses	0.46/0.51	0.50/0.53	0.78/0.80	0.85/0.862

In Fig.13, the yellow line and the purple line present DR/FPPI by the single-chain θ -HMM and L -HMM, respectively. Their DR/FPPI are much less than that by PSM-CHMM. CHMM can improve the detection accuracy since CHMM considerate the feature coupling effects. Table 2 is DR comparisons when FPPI = 0.3/0.4. The index of DR is much higher than the other three methods. So, PSM-CHMM improves the accuracy of object detection. Fig. 14 presents some examples of detection results for the apple logo, giraffe, bottle, swan, and horse, where the contour polygon model is given in first column, the second column

is the test images, the third column is contour extraction results and the fourth column is detection results.

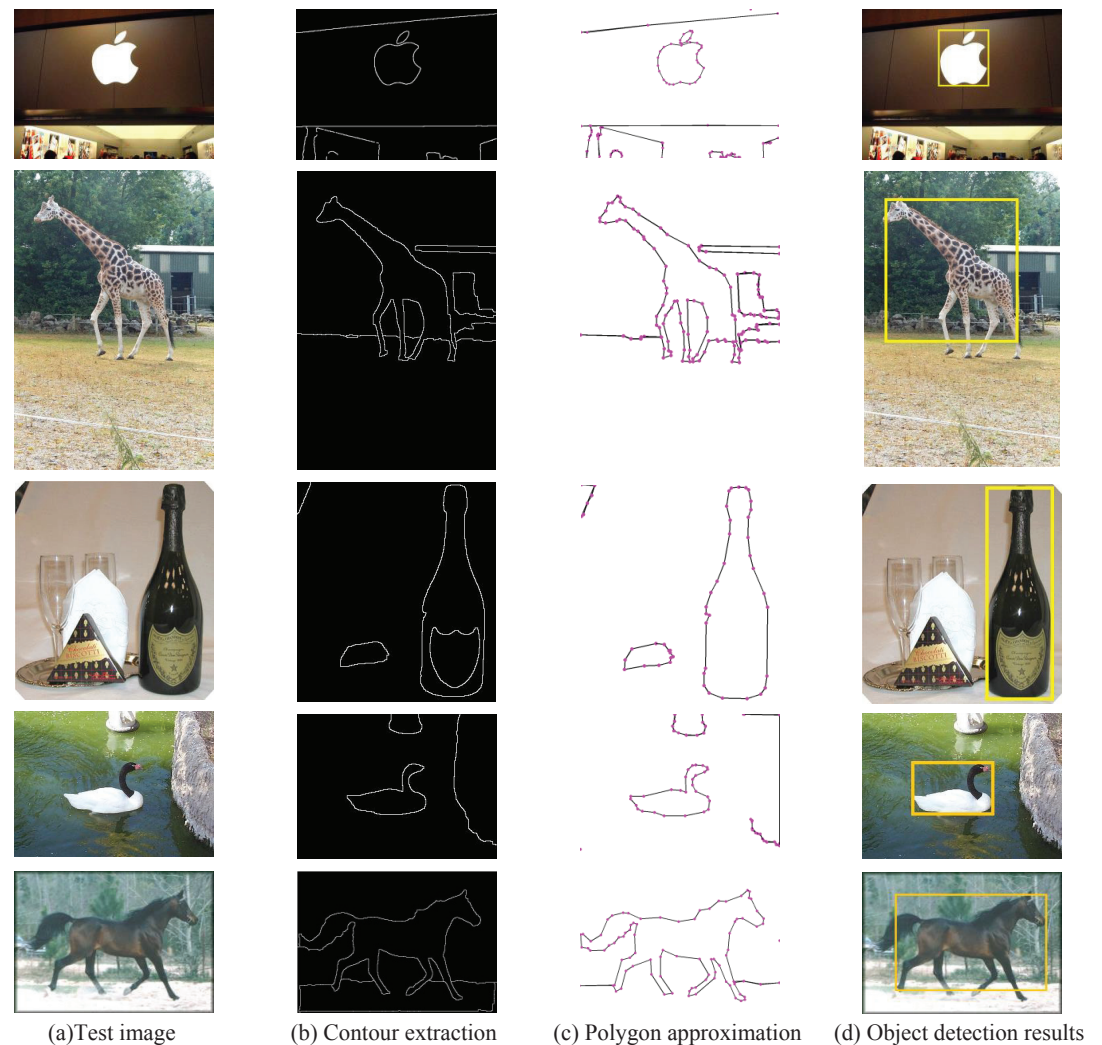


Figure 14. Some examples of detection results.

4. Conclusions

Since SM algorithm is sensitive to the object scale variance and splitting starting point, PSM polygon approximation algorithm is proposed to extract the object contour features. PSM algorithm has some advantages. The contour corner is used as the starting point for the contour piecewise approximation to reduce the sensitivity of the contour segment on the starting point, and both the distance ratio and the arc length ratio instead of the distance error are used as the iterative stop condition to improve the robustness to the object scale variance. PSM algorithm is applied to bat included in the MPEG-7 data set to verify the performance. In different scales and rotated experiments, the index of polygon vertices keeps almost invariant for PSM algorithm. The length and angle of the line segment by PSM algorithm are the two major elements that determine the shape of the contour polygon. The two features have a strong coupling relationship, but the changes of the two variables are random and asynchronous. CHMM with two contour features is constructed to improve the accuracy of object detection and anti-noise robustness. The ETHZ Shape Classes and INRIA Horses data sets are selected to verify the performance for PSM-CHMM in the

experiment. The indexes of DR/FPPI and DR for 0.3/0.4 FPPI indicate that PSM-CHMM has a much better performance than the other three methods.

Author Contributions: Conceptualization, S.Z. and Y.H.; methodology, Y.H.; software, Y.H.; validation, S.Z. and Y.H.; formal analysis, S.Z.; investigation, S.Z.; resources, Y.H.; data curation, S.Z.; writing—original draft preparation, Y.H.; writing—review and editing, S.Z.; visualization, S.Z.; supervision, Y.H.; project administration, Y.H.; All authors have read and agreed to the published version of the manuscript.

Funding: This research was funded by the Natural Science Foundation of Fujian under project 2019H0007.

Informed Consent Statement: Not applicable.

Data Availability Statement: Not applicable.

Acknowledgments: Not applicable.

Conflicts of Interest: The authors declare no conflict of interest.

References

1. Tsai, P.-F.; Liao, C.-H.; Yuan, S.-M. Using Deep Learning with Thermal Imaging for Human Detection in Heavy Smoke Scenarios. *Sensors* **2022**, *22*, 5351.
2. Yang, J.; Wang, L.; Li, Y. Feature Refine Network for Salient Object Detection. *Sensors* **2022**, *22*, 4490.
3. Wei, H.; Yu, Q.; Yang, C. Minhas, H. N. Shape-based object recognition via Evidence Accumulation Inference. *Pattern Recognit. Lett.* **2016**, *77*, 42–49.
4. Giang, T.T.H.; Khai, T.Q.; Im, D.-Y.; Ryoo, Y.-J. Fast Detection of Tomato Sucker Using Semantic Segmentation Neural Networks Based on RGB-D Images. *Sensors* **2022**, *22*, 5140.
5. Wei, H.; Yang, C.; Yu, Q.; Minhas, H. N. Efficient graph-based search for object detection. *Elsevier Science Inc* **2017**, *385*, 395–414.
6. Wei, H.; Yang, C.; Yu, Q. Contour Segment Grouping for Object Detection. *J. Vis. Commun. Image Represent.* **2017**, *48*, 292–309.
7. Ferrari, V.; Fevrier, L.; Jurie, F. Groups of Adjacent Contour Segments for Object Detection. *IEEE Trans. Pattern Anal. Mach. Intell.* **2008**, *30*, 36–51.
8. Martin, E. M.; Pobil, APD. Object Detection and Recognition for Assistive Robots. *IEEE Robot. Autom. Mag.* **2017**, *99*, 1–1.
9. Zhang, G. M.; Xu, J. Y.; Liu, J. X. A New Method for Recognition Partially Occluded Curved Objects under Affine Transformation. In Proc. 10th International Conference on Intelligent Systems and Knowledge Engineering, Taiwan, 2016. pp.456–461.
10. Huang, C.; Han, T. X.; He, Z.; Cao, W. Constellational contour parsing for deformable object detection. *J. Vis. Commun. Image Represent.* **2016**, *38*, 540–549.
11. Riemenschneider, H.; Donoser, M.; Bischof, H. Using partial edge contour matches for efficient object category localization. In Proc. 11th European Conference on Computer Vision, Crete, Greece 2010. pp.29–42.
12. Ma, L.; Jiang, B. Edge Grouping with a Novel Shape Model for Object Detection. In Proc. Seventh International Conference on Image and Graphics, Qingdao, China, 2013. pp.186–191.
13. Ramer, U. An iterative procedure for the polygonal approximation of plane curves. *Comput. Graph. Image Process.* **1972**, *1*, 244–256.
14. Qian, W. G.; Liu, X. Z. Detection Algorithm of Image Corner Based on Contour Sharp Degree (in Chinese). *Comput. Eng.* **2008**, *34*, 202–204.
15. Guerrero-Peña, F. A.; Vasconcelos, GC. Object recognition under severe occlusions with a hidden Markov model approach. *Pattern Recognit. Lett.* **2017**, *86*, 68–75.
16. Guerrero-Peña, F. A.; Vasconcelos, GC. Search-space sorting with hidden Markov models for occluded object recognition. In IEEE 8th International Conference on Intelligent Systems, Sofia, Bulgaria, 2016.
17. Bicego, M.; Murino, V. Investigating Hidden Markov Models' capabilities in 2D shape classification. *IEEE Trans. Pattern Anal. Mach. Intell.* **2004**, *26*, 281–286.
18. Brand, M.; Oliver, N.; Pentland, A. Coupled hidden Markov models for complex action recognition. In Proc. the 1997 Conference on Computer Vision and Pattern Recognition, Washington, DC, USA, 1997. pp.994–999.
19. Zhou, H.; Chen, J.; Dong, G. Bearing fault recognition method based on neighbourhood component analysis and coupled hidden Markov model. *Mech. Syst. Signal Proc.* **2016**, *66*, 568–581.
20. Arbelaez, P.; Maire, M.; Fowlkes, C.; Malik, J. Contour detection and hierarchical image segmentation. *IEEE Trans. Pattern Anal. Mach. Intell.* **2011**, *33*, 898–916.
21. Xiao, W. B. *Study on Coupled Hidden Markov Model Based Rolling Element Bearing Fault Diagnosis and Performance Degradation Assessment*; Publisher: Shanghai Jiao Tong University, Shanghai, 2011.